ARTICLE

Stretching and Solvency of Charged Cellulose Chains

Shannon M. Notley†

Department of Applied Mathematics, Research School of Physics and Engineering, Australian National University, Canberra 0200 ACT, Australia

ABSTRACT The transition between good and poor solvency conditions was studied for cellulose interacting in an aqueous environment as a function of the pH and ionic strength as well as for cellulose with weakly ionizable grafted groups. For uncharged cellulose, poor solvent conditions were observed for a pH range of 4−10 and an ionic strength between 0.1 and 10 mM, as demonstrated by the characteristic constant force plateau in the single-molecule force spectroscopy data as a function of the polymer extension. The magnitude of the force plateaus was quantized, indicating that on occasion more than a single cellulose chain was stretched into solution. Charged cellulose was also studied with a transition from poor to good solvency observed by an increase in the pH of the solution well above the pK_a of the carboxyl groups. This transition was characterized by a fundamental change in the form of the force data as a function of extension from the constant force plateau (poor solvent conditions) to the nonlinear increase in adhesion due to elastic stretching (good solvent conditions). Using this single-molecule technique, the Kuhn length of cellulose was determined to be 3.8 Å from the fit to a freely jointed chain model. Furthermore, the loop distribution under the good solvent conditions was studied as a function of the pH and ionic strength. The distribution became more compact as the influence of the charged groups was reduced through an increase in the screening or a reduction in the charge density, with chain association dominating because of strong hydrogen bonding.

KEYWORDS: cellulose • surface forces • adhesion • good solvent • poor solvent • single molecule force spectroscopy • loop distribution

INTRODUCTION

There has been renewed interest in naturally occurring biopolymers such as cellulose for materials applications because of their relative abundance, economic viability, and environmentally sustainable production (1). In order to extend the use of this important resource chiefly found in the load-bearing components of plant cell walls, a further understanding of the interaction and compatibility of cellulose with other materials, both organic and inorganic in nature, and in a variety of media such as air and aqueous solution and in other solvents must be gained.

Understanding both the inter- and intramolecular interactions between cellulose chains will provide valuable insight into the mechanisms of adhesion so important to many natural systems such as in the plant cell wall and also industrial systems such as paper and textiles (2–4). Previous studies into the adhesion between cellulose surfaces have tended to focus on macroscopic or ensemble measurements (5,6). The Hamaker constant, a measure of the apparent attractive dispersion forces between cellulose surfaces, has been determined from spectroscopic ellipsometry and directly measured using colloidal probe microscopy (7, 8). The thermodynamic work of adhesion has also been determined using a JKR-type microadhesion apparatus (9). Furthermore, a measure of the adhesive interactions between cellulose-based materials has been performed using both tensile and peel-testing procedures (10, 11). With all of these techniques, significant uncertainties in the measured values exist chiefly because of the poorly defined interaction geometry due to roughness. The conformation of individual cellulose chains at the interface and the relative contribution of these single macromolecules to the measured adhesive energy remain largely unknown.

The adhesion and stretching of single cellulose chains in an aqueous environment are yet to be fully investigated, and indeed few experimental techniques exist to directly probe statistically improbable events such as polymer loop segment bridging. One such available technique, often termed single-molecule force spectroscopy, has been used in the investigation of the conformation of adsorbed polymers or polyelectrolytes at an interface (12–14) and for polysaccharides specifically (15–17). Bridging polymer loops are stretched as the two surfaces are separated under well-defined solvent conditions. The corresponding force−separation curve generated from the experiment is characteristic of the solvent quality, either good (Langevin shape indicative of a dominant elastic stretching contribution) or poor (so-called Plateau shape due to "unzipping" of the polymer segments from the substrate) (18, 19). The Langevin profile arises from the energy required to stretch all polymer segments into the trans configuration and hence maximize polymer−solvent interactions. However, the Plateau profile, characteristic of poor solvency, is due to the removal of sequential monomer segments from the effectively better solvent conditions in the globular phase, which for all monomer segments requires the same energy,

† E-mail: shannon.notley@anu.edu.au.
Received for review February 12, 2009 and accepted May 5, 2009
DOI: 10.1021/am900096c

Published on Web 05/14/2009

in principle. Thus, it has been well established that the form of the force–distance data upon separation of the surfaces as single polymer chains are stretched is indicative of the solvent quality for a given polymer–solvent system. Indeed, the switching from a good to a poor solvent for single polymer chains upon action of an external stimulus can be probed using this experimental technique. Possibly the best example of this effect is seen for poly(*N*-isopropylacrylamide) in water, with the external stimulus being temperature here (20). Senden et al. showed that below the lower critical solution temperature (LCST) a Langevin force profile was apparent, in agreement with polyNIPAM under good solvent conditions. However, above the LCST, the Plateau force profile was observed, characteristic of poor solvency and demonstrating that the single-molecule stretching experiments are highly sensitive in probing solvency change.

Other stimuli that may be used to induce a change in solvency include the pH (21) and ionic strength (20), particularly when the single molecules under investigation are polyelectrolytes. Here, the stretching of single cellulose chains into aqueous solution is studied using a scanning-probe-based single-molecule technique, with and without weakly ionizable groups grafted to the macromolecular backbone. Previous studies have suggested some limited affinity of cellulose for water based upon surface force measurements on the approach of two cellulose surfaces because of the presence of an observed steric interaction (3, 22–24), while in other studies, these steric layers are not present (3, 8, 25).

Previous single-molecule stretching experiments involving cellulose have indicated, for the most part, poor solvency under a range of aqueous conditions; however, this largely depends on the preparation method of the cellulose surface (15–17). The shape of the force–separation curve will provide insight into the solvency of cellulose in aqueous solutions. This present study looks at the effect of the presence of charged groups on the observed interaction profile and hence infers the solvency of cellulose in aqueous solution. The carboxylic acid groups grafted to the molecular backbone should have the 2-fold effect of reducing intermolecular hydrogen-bonding interactions between crystalline cellulose regions as well as improving the solvophilicity of the cellulose chains when these charged groups are dissociated. Furthermore, the strength of inter- and intrachain association may be probed by altering the solution conditions, in particular, the pH and ionic strength, which will influence the charge dissociation and hence the swelling of these cellulose films (4, 26).

EXPERIMENTAL SECTION

Cellulose Film Preparation. Cellulose thin films supported on an oxidized silicon wafer were prepared according to a previously described method (27). A 0.5% (w/w) solution of cellulose in *N*-methylmorpholine oxide (NMMO) was prepared by dissolving 0.1 g of dissolving-grade pulp (Domsjo Fabriken, Västernorrland, Sweden) in 20 g of the solvent supplied as a 50% (v/v) NMMO/water solution (Sigma Aldrich, Madion, WI) at 110 °C. After approximately 1 h, the cellulose was completely dissolved, at which point the solution was diluted with dimethyl sulfoxide to give a final volume of 50 mL. The cellulose solution was spin-coated onto a smooth oxidized silicon wafer pretreated with poly(vinylamine) (BASF, Ludwigsafen, Germany). The spinning parameters were 1500 rpm for 45 s, which produced cellulose thin films of approximately 40 nm as measured by ellipsometry.

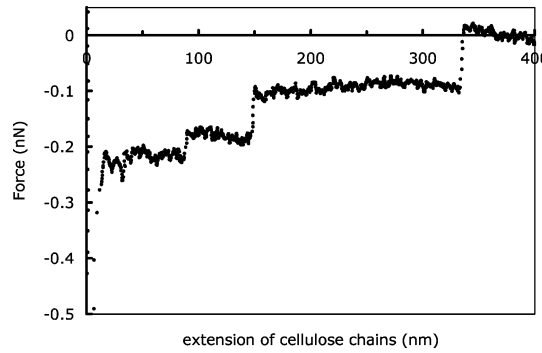

FIGURE 1. Force–distance curve upon separation of a silica nitride tip from an uncharged cellulose surface at pH 4 and a 1 mM background electrolyte concentration. Constant force plateaus are observed at approximately integer multiples of 80 ± 5pN.

Thin films of the semicrystalline cellulose of two different charges were, furthermore, prepared: the first was simply the native charge of the dissolving-grade pulp, and the second was cellulose with grafted carboxymethyl groups prepared according to the method of Walecka (28). The charge on the cellulose was measured using conductometric titration and found to be 425 μequiv/g or a degree of substitution of 7%. Previous studies have shown that the carboxylic acid groups are retained in the prepared surfaces (25, 29).

Single-Molecule Force Experiments. Force measurements were performed in aqueous solutions of NaCl (Sigma, Australia) with the pH adjusted using an appropriate amount of either HCl or NaOH. All solutions were prepared with Milli-Q water and used within 24 h.

A multimode scanning probe microscope (Veeco, Fremont, CA) was used for the single-molecule force experiments. A silicon nitride cantilever (Veeco) with a tip radius of 5–10 nm and a spring constant of 0.06 N/m was used after calibration using the thermal noise method (30). For each of the solution conditions tested in this study, a minimum of 100 force–extension curves were measured, with the data presented here representative for each condition. The maximum applied load was 20 nN, and the pulling velocity was 400 nm/s.

RESULTS AND DISCUSSION

Figure 1 shows a typical force–distance curve upon separation of a silicon nitride atomic force microscopy (AFM) cantilever from a spin-coated cellulose film in an aqueous electrolyte solution with the pH adjusted to 4 and a 1 mM background electrolyte concentration. Cellulose, under these conditions, would have a minimal amount of charged groups from possible degradation or hydrolysis reactions and as such may be expected to behave as close to the naturally occurring material as possible. Indeed, in previous surface force measurements using similarly prepared cellulose thin films, the attractive van der Waals interaction dominated and no surface potential was measured under the same solution conditions (8).

In Figure 1, a number of Plateau events are observed upon separation of the tip away from the cellulose substrate, indicating poor solvency of cellulose under these solution

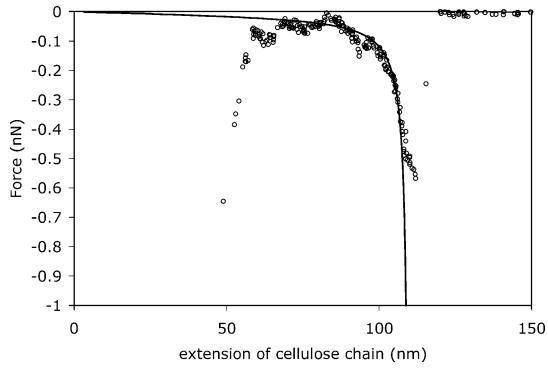

FIGURE 2. Langevin-type interaction curves measured between a charged cellulose film and the Si_3N_4 tip at pH 8 and a 0.1 mM NaCl background electrolyte solution. Force−extension curve fit to a FJC model for charged cellulose at pH 8 and 0.1 mM ionic strength. Fitting parameters are a Kuhn length of 3.8 Å and a contour length of 112 nm.

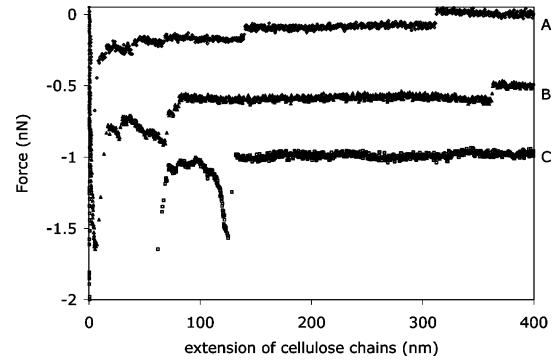

FIGURE 3. Force−distance curve of charged cellulose pulled into solution. The curves are offset for clarity of presentation. Curves a−c show charged cellulose as a function of decreasing ionic strength at pH 8 from 10 mM to 1 mM to 0.1 mM.

conditions. The constant force depth as a function of the polymer chain extension arises because of the effective "unzipping" of monomer units away from their anchoring points at the interface. Indeed, in the pH range of 4−10 and with an ionic strength of 0.1−100 mM NaCl, only the Plateau-type force−separation curves were measured. These constant-force plateaus are observed in approximately 40% of the force−separation curves; however, the significantly larger primary adhesion at short surface separations is always present. Interestingly, the magnitude of the plateaus is quantized, indicating that multiple chains are pulled into the poor solvent. The force plateaus are approximately integer multiples of the lowest observed force magnitude of 80 ± 5pN. In the study of Radtchenko et al., force plateaus of similar magnitude were also observed; however, they suggested the presence of a plateau in the force magnitude of 40 pN followed by plateau values at the even integer multiples (17). Here, no evidence of this plateau was observed. If the cellulose polymer chain is approximated as a cylinder (20), then the force required to pull the chain into a poor solvent is given by $F = 2\pi r\gamma$, where r is the molecular radius and γ is the surface energy of cellulose (31), taken to be 54.5 mJ/m^2. When this is applied to the force plateau of 80 pN, the radius is calculated to be 2.3 Å or of the molecular dimensions as expected for single linear polymer chains.

Cellulose films with grafted charged groups were also prepared to investigate the possibility of tuning the solvency from poor to good depending on the solution conditions. Figure 2 shows the interaction between the Si_3N_4 tip and a cellulose film, where 7% of the monomers have had carboxyl substituents grafted in place of a hydroxyl group. The carboxymethylated cellulose now behaves as a weak polyelectrolyte and, as such, the polymer solvency will be highly influenced by the solution pH and ionic strength. Under solution conditions where the charge on the cellulose is maximized, such as in, for example, high pH and low-to-intermediate ionic strengths, the observed interaction is now of the Langevin type. The representative force−interaction curve in Figure 2 demonstrates that only a small amount of charge is sufficient to alter the solvency of the cellulose chains from poor to good.

Previously, attempts have been made to fit the nonlinear interaction curves using different models based around the Langevin function (32–34) with the Kuhn length and contour length as fitting parameters. These theories have, furthermore, been extended to incorporate contributions to the overall force from bond length and bond angle deformations. However, in many cases, the simplified freely jointed chain (FJC) or wormlike chain suffices, particularly for low force extensions, where the bridging interactions of the polymer with the tip or surface are weak. Figure 2 shows an example of the good solvent interaction of cellulose with the best fit using the FJC model, the fitting parameters employed here were a Kuhn length of 3.8 Å and a contour length of 112 nm, under these solution conditions. This experimentally obtained Kuhn length is in good agreement with measurements for other polysaccharides using a similar single-molecule stretching technique (35) and suggests that the presence of a minimal number of grafted charge groups on the cellulose polymer does not significantly increase the stiffness of the polymer chain through intramolecular charge repulsions and electrostatic contributions to the Bjerrum length. It must be stated, however, that there is significant scatter in the fitted values for the Kuhn length determined using this AFM-based technique, with molecular dynamics simulations perhaps a more reliable method for calculating the persistence lengths of polymers and polyelectrolytes. This is particularly important because the Kuhn length measured using this single-molecule technique is significantly less than that determined from simulation and light scattering because of the scale dependence of the electrostatic persistence length, particularly under high force (36, 37).

At pH 8, which is significantly greater than the pK_a of the charged carboxyl groups, the solvency of the individual chains was probed as a function of the ionic strength. Figure 3 shows representative interaction curves for the charged cellulose chains with decreasing NaCl concentration. As the ionic strength is increased up to 10 mM (curve a), the Plateau force−separation shape is observed. Furthermore, a combination of the two is seen at an intermediate ionic strength of 1 mM (curve b). Increasing the ionic strength of the solution will screen the charges on the cellulose polymer chains, effectively reducing the persistence length and causing a rod-to-globule transition. Thus, the solvency of the

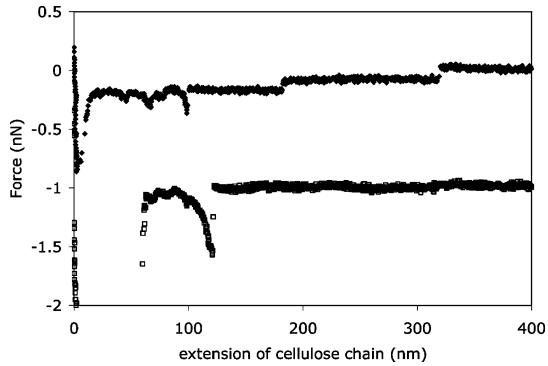

FIGURE 4. Force–distance curve of charged cellulose pulled into solution as a function of the pH at a constant ionic strength of 0.1 mM. The force profile changes from Plateau events to good solvency as the pH is increased. The curves are offset for clarity. Closed symbols are for pH 4, and open symbols are for pH 8.

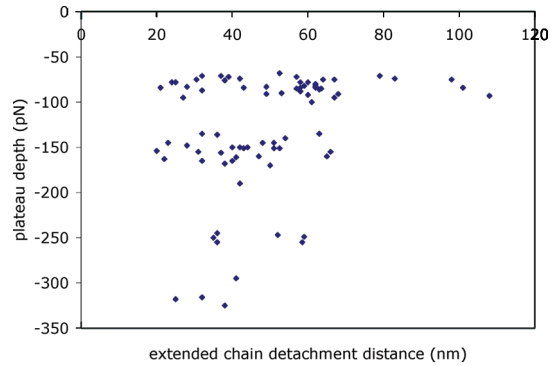

FIGURE 5. Combined Plateau events for both uncharged and charged cellulose under poor solvent conditions. The Plateau events are quantized with the depth equivalent even after the introduction of grafted carboxylic acid groups. A total of 80 Plateau events are shown, with the depth measured as a function of the separation where the cellulose chain ruptures.

charged cellulose at high pH is very sensitive to the ionic strength of the solution into which it is stretched. At an intermediate ionic strength of 1 mM NaCl, the combination of the two solvency regimes is interesting. Such behavior is consistent with that reported by Chatellier et al., who suggest that the Debye screening length is the critical factor in determining the onset of the Plateau region (18). However, in their study, the Plateau region began at surface separations greater than one Debye length, in agreement with predictions based upon scaling arguments. Here in this study, for a salt concentration of 1 mM, the Debye length should be on the order of 9 nm, but Figure 4 shows that there is still significant nonlinearity at surface separations much greater than this, which is somewhat surprising. It should be noted though that the form of the force curve is rather different from what may be expected for a purely good solvent interaction, which may be fit with a characteristic Langevin function. The shorter Debye length associated with a further increase of the ionic strength up to 10 mM suggests, within the force and separation resolutions of this single-molecule stretching technique using the AFM, that the charged cellulose polyelectrolyte molecules should essentially behave as their uncharged analogues. Figure 3 confirms that for ionic strengths of 10 mM and greater only the Plateau-type poor solvent interactions are observed.

The carboxylic groups grafted to the cellulose are weakly ionizable. Therefore, it is expected that there may be a possibility to tune the solvency of the weak polyelectrolyte molecules by altering the solution pH. With the charged cellulose at a high ionic strength of 10 mM, all of the force curves indicate poor solvency under the pH range of 4–10 studied here. At a lower ionic strength of 0.1 mM, if the pH of the solution is reduced to on the order of a pK_a of the charged carboxyl groups at pH 4–5, then the force–distance interaction is dominated by the poor solvent interaction, as shown in Figure 4. However, with an increase of the solution pH beyond 5, the good solvent regime can be observed.

Using this single-molecule stretching experimental technique, it is, hence, possible to predict the onset of poor solvent conditions as a function of the pH and ionic strength based upon the force–distance interaction profile. Furthermore, the presence of charged groups will play a significant role in the effective solvency of cellulose. For uncharged cellulose, comparable to the naturally occurring material, only the Plateau-type force curves were observed, indicating that cellulose has a poor affinity for aqueous solvents. However, when the charge on the cellulose polymer is maximized through carboxymethylation, the solvency can be improved. Previous studies examining the force response of polysaccharides have only focused on this good solvency regime where chair–boat transitions have been observed (12, 35, 38). No force-induced twisting of the pyranose ring was observed here, in agreement with predictions from ab initio calculations of the separation of glycosodic oxygen atoms (35) as well as direct force measurements of highly charged carboxymethylated cellulose (38, 39).

Figure 5 shows a compilation of the Plateau-type interaction curves for the various solution conditions where the cellulose chains are stretched into a poor solvent. This figure shows that the magnitude of the force Plateau is the same for the various solution conditions and charges on the cellulose. This suggests that the presence of carboxyl groups does not significantly alter the molecular dimensions of the polymer or the surface energy. The surface energy of naturally occurring cellulose is dominated by the dispersive component (2) so that the addition of only a small amount of charge will increase the polar component only slightly.

This single-molecule stretching technique may also be used to derive the loop distribution of the macromolecules at the interface by statistically investigating the extension of the cellulose chains. Senden and co-workers derived the theoretical loop distribution through simple scaling arguments (40). On the basis of the earlier work of de Gennes (41–43) and supported by the theory of Guiselin (44), they showed that for neutral polymers two regimes could be described depending upon the penetration of the AFM tip into the interfacial polymer layer, with the assumption that the tip does not significantly alter the adsorbed layer conformation. For the first regime, where the correlation length of the semidilute solution is greater than the surface separation and the monomer volume fraction varies as a function of the distance, the loop distribution, $S(n)$, scales with the length of the chain, n, according to $S(n) \sim n^{-11/5}$.

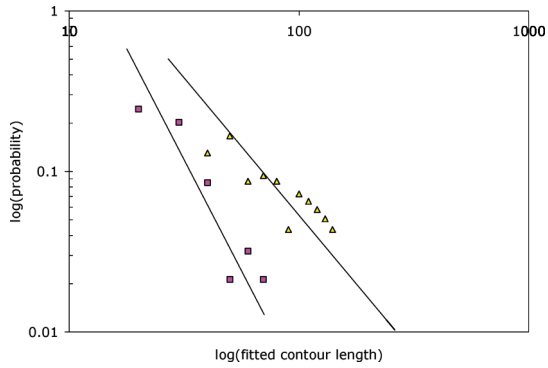

FIGURE 6. Loop distribution of charged cellulose as a function of the pH in a background electrolyte of NaCl with a concentration of 0.1 mM. Closed squares are pH 5, and open triangles represent pH 9.

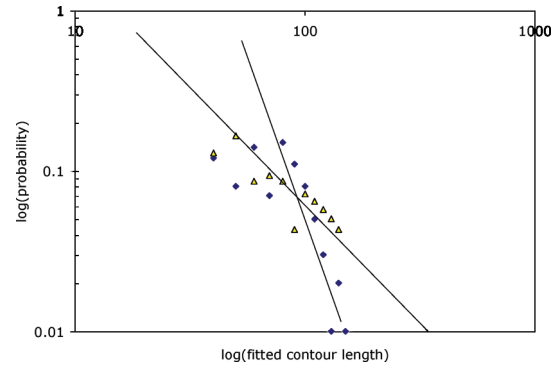

FIGURE 7. Loop distribution of charged cellulose as a function of the ionic strength of the NaCl electrolyte solution at a constant pH of 9. Closed diamonds are 1 mM salt concentration, and open triangles are 0.1 mM salt concentration.

However, if it is assumed that the AFM tip does not penetrate the layer to any great extent such that the monomer volume fraction is constant and the surface separation is greater than the correlation length, the loop distribution scales as $S(n) \sim n^{-3/2}$. The theory of Guiselin, also based around scaling arguments, however derived from considering a polymer melt in contact with a hard wall in the absence of any free polymer in solution, a so-called "Guiselin brush", confirms this power law relationship of $S(n) \sim n^{-3/2}$ for the distribution of loops. Thus, for neutral polymers in the absence of significant intrachain association and in good solvent conditions, a plot of the log(frequency) of events versus log(contour length) should yield a slope of $-3/2$, which has been experimentally verified (37, 40).

Here, the force–extension curves for the charged cellulose under good solvent conditions were subjected to this above-described loop distribution analysis. Figure 6 shows the loop distribution for the charged cellulose at an ionic strength of 0.1 mM at pH 5 and 9. Under these conditions, a previous study showed that the surface potential of similarly charged cellulose films increased significantly with increasing pH (4). It is, hence, expected that the loop distribution should be somewhat different as a function of the pH because the higher charge should result in more extended polymer segments. However, it should also be borne in mind that no steric force was observed in the previous surface forces study and that the charged cellulose surface itself should be considered to be more like a polyelectrolyte gel, with many polymer loops and segments accessible to an AFM tip, than like a discrete interface.

In Figure 6, if the data for loop segments at very short surface separations are ignored, the frequency of the loops decays with distance in a linear fashion. The reason for neglecting the data at short separation is due to the difficulty in determining the point of zero separation in an AFM force experiment, particularly when polymers are at the interface. Zero separation is defined as the onset of the constant compliance region on the force–distance curve, that is, where a linear motion of the surface results in a linear output of the detector (45). As such, for the case of polymeric surfaces, there may be a significant error of up to a few nanometers in the defined zero separation between the tip and surface due to pinned polymer chains. This error in the surface separation will hence have a far greater impact on the measurement of loops of shorter chains than longer chains.

Figure 6 shows that there is a significant difference between the loop distributions at pH 5 and 9. Interestingly, the slope at pH 9 is close to that predicted from scaling theory for a neutral polymer in a good solvent, $-3/2$. This suggests that while the presence of a minimal number of charged groups on the cellulose macromolecules gives rise to a good solvent interaction, the charged cellulose behaves more similarly to a neutral polymer than a rigid rodlike polyelectrolyte, where the observed slope will be significantly less than $-3/2$ (40). It is likely that, at pH 9 and 0.1 mM ionic strength, there is only a sufficient charge on the cellulose to overcome the strong intra- and intermolecular hydrogen bonding common in cellulosic systems (10, 11, 46). This is supported by the data for the loop distribution at pH 5. The slope increases for pH 5, indicating that as the charges on the cellulose are neutralized the intermolecular hydrogen bonding begins to dominate over the electrostatic component, resulting in a quicker decay for the observed loop distribution due to chain association.

The loop distribution was also measured as a function of the ionic strength and is shown in Figure 7. The electrostatic contribution to the persistence length is screened as the background electrolyte concentration is increased. This causes a collapse of the extent of the loops into solution, and hence there is a significant increase in the slope of the distribution, as shown in Figure 7, at the higher ionic strength of 1 mM. Higher ionic strengths resulted in poor solvent interaction.

CONCLUSIONS

From the force–extension profiles under the aqueous solution conditions studied here, uncharged cellulose is always pulled into a poor solvent, as demonstrated by the Plateau events. However, when charged groups are introduced onto the cellulose backbone, the solvency of the individual polymeric chains can be tuned, depending on the charge density and solution conditions, which include vari-

able pH and ionic strength. Under poor solvent conditions, the depth of the Plateau events indicates that single molecules are bridging the surface. Furthermore, the presence of grafted carboxyl groups did not change the magnitude of the constant force plateau values when the solution conditions favored poor solvency. For good solvent conditions, the Langevin force−extension curves may be fit using a FJC model with a Kuhn length on the order of ∼3.8 Å. Under these good solvent conditions, the loop distribution of cellulose at the solid−liquid interface was determined and found to agree well with scaling theory predictions for conditions when the charged cellulose may be expected to be fully dissociated and with minimal screening due to the background electrolyte. A reduction in the pH and therefore the charge density or an increase in the ionic strength resulted in a more compact loop distribution presumably because of the strong intra- and interchain association of hydrogen bonding becoming dominant over the electrostatic repulsion between charged groups. Hence, using this single-molecule stretching technique, the solvency of cellulose chains as a function of the charge may be studied both qualitatively in terms of the force−extension profiles and quantitatively in terms of the polymer parameters.

Acknowledgment. Tim Senden and Vince Craig, Australian National University, are gratefully acknowledged for helpful discussions and continued guidance.

REFERENCES AND NOTES

(1) Ragauskas, A. J.; Williams, C. K.; Davison, B. H.; Britovsek, G.; Cairney, J.; Eckert, C. A.; Frederick, W. J.; Hallett, J. P.; Leak, D. J.; Liotta, C. L.; Mielenz, J. R.; Murphy, R.; Templer, R.; Tschaplinski, T. *Science* **2006**, *311*, 484–489.
(2) Eriksson, M.; Notley, S. M.; Wagberg, L. *Biomacromolecules* **2007**, *8*, 912–919.
(3) Notley, S. M.; Eriksson, M.; Wagberg, L.; Beck, S.; Gray, D. G. *Langmuir* **2006**, *22* (7), 3154–3160.
(4) Notley, S. M. *Phys. Chem. Chem. Phys.* **2008**, *10*, 1819–1825.
(5) Rutland, M. W.; Carambassis, A.; Willing, G. A.; Neuman, R. D. *Colloids Surf., A* **1997**, *123*, 369–374.
(6) Kontturi, E.; Tammelin, T.; Ošterberg, M. *Chem. Soc. Rev.* **2006**, *35* (12), 1287–1304.
(7) Bergström, L.; Stemme, S.; Dahlfors, T.; Arwin, H.; Ödberg, L. *Cellulose* **1999**, *6*, 1–13.
(8) Notley, S. M.; Pettersson, B.; Wagberg, L. *J. Am. Chem. Soc.* **2004**, *126* (43), 13930–13931.
(9) Rundlof, M.; Karlsson, M.; Wagberg, L.; Poptoshev, E.; Rutland, M.; Claesson, P. *J. Colloid Interface Sci.* **2000**, *230*, 441–447.
(10) *Wood and Cellulosic Chemistry*; Hon, D. N.; Shiraishi, N., Eds.; Marcel Dekker: New York, 1991.
(11) Sjostrom, E. *Wood Chemistry: Fundamental and Applications*, 2nd ed.; Academic Press: New York, 1993.
(12) Rief, M.; Oesterhelt, F.; Heymann, B.; Gaub, H. E. *Science* **1997**, *275*, 1295.
(13) Li, H.; Liu, B.; Zhang, X.; Gao, C.; Shen, J.; Zou, G. *Langmuir* **1999**, *15*, 2120–2124.
(14) Hugel, T.; Grosholz, M.; Clausen-Schaumann, H.; Pfau, A.; Gaub, H.; Seitz, M. *Macromolecules* **2001**, *34*, 1039–1047.
(15) Leporatti, S.; Sczech, R.; Riegler, H.; Bruzzano, S.; Storsberg, J.; Loth, F.; Jaeger, W.; Laschewsky, A.; Eichhorn, S.; Donath, E. *J. Colloid Interface Sci.* **2005**, *281*, 101–111.
(16) Morris, S.; Hanna, S.; Miles, M. J. *Nanotechnology* **2004**, *15*, 1296–1301.
(17) Radtchenko, I. L.; Papastavrou, G.; Borkovec, M. *Biomacromolecules* **2005**, *6*, 3057–3066.
(18) Chatellier, X.; Senden, T. J.; Joanny, J.-F.; Di Meglio, J.-M. *Europhys. Lett.* **1998**, *41* (3), 303–308.
(19) Senden, T. J.; Di Meglio, J.-M.; Auroy, P. *Eur. Phys. J. B* **1998**, *3*, 211–216.
(20) Haupt, B. J.; Senden, T. J.; Sevick, E. M. *Langmuir* **2002**, *18*, 2174–2182.
(21) Sonnenberg, L.; Parvole, J.; Borisov, O.; Billon, L.; Gaub, H. E.; Seitz, M. *Macromolecules* **2006**, *39*, 281–288.
(22) Osterberg, M.; Claesson, P. M. *J. Adhes. Sci. Technol.* **2000**, *14*, 603–618.
(23) Carambassis, A.; Rutland, M. W. *Langmuir* **1999**, *15* (17), 5584–5590.
(24) Neumann, R. D.; Berg, J. M.; Claesson, P. M. *Nord. Pulp Pap. Res. J.* **1993**, *8*, 96–104.
(25) Notley, S. M.; Wagberg, L. *Biomacromolecules* **2005**, *6* (3), 1586–1591.
(26) Freudenberg, U.; Zimmerman, R.; Schmidt, K.; Behrens, S. H.; Werner, C. *J. Colloid Interface Sci.* **2007**, *309*, 360–365.
(27) Gunnars, S.; Wågberg, L.; Cohen-Stuart, M. A. *Cellulose* **2002**, *9*, 239–249.
(28) Walecka, J. A. *TAPPI J.* **1956**, *39*, 458–463.
(29) Fält, S.; Wågberg, L.; Vesterlind, E. L. *Langmuir* **2003**, *19*, 7895–7903.
(30) Hutter, J. L.; Bechhoefer, J. *Rev. Sci. Instrum.* **1993**, *64*, 1868–1873.
(31) van Oss, C. J. *Interfacial Forces in Aqueous Media*; Marcel Dekker: New York, 1994.
(32) Smith, S. B.; Finzi, L.; Bustamante, C. *Science* **1992**, *258*, 1122.
(33) Smith, S. B.; Cui, Y.; Bustamante, C. *Science* **1996**, *271*, 795–799.
(34) Bustamante, C.; Marko, J. F.; Siggia, E. D.; Smith, S. *Science* **1994**, *265*, 1599.
(35) Marszalek, P. E.; Oberhauser, A. F.; Pang, Y. P.; Fernandez, J. M. *Nature* **1998**, *396*, 661–664.
(36) Netz, R. R. *Macromolecules* **2001**, *34*, 7522–7529.
(37) Papastavrou, G.; Kirwan, L. J.; Borkovec, M. *Langmuir* **2006**, *22*, 10880–10884.
(38) Li, H.; Rief, M.; Oesterhelt, F.; Gaub, H. E.; Zhang, X.; Shen, J. *Chem. Phys. Lett.* **1999**, *305*, 197–201.
(39) Li, H. B.; Rief, M.; Oesterhelt, F.; Gaub, H. E. *Adv. Mater.* **1998**, *10*, 316–319.
(40) Senden, T. J.; Di Meglio, J. M.; Silberzan, I. *C. R. Acad. Sci. Paris Ser. IV* **2000**, 1143–1152.
(41) de Gennes, P.-G. *Macromolecules* **1981**, *14*, 1637–1644.
(42) de Gennes, P.-G. *Macromolecules* **1982**, *15*, 492–500.
(43) de Gennes, P. G. *C. R. Acad. Sci. Paris, Ser. II* **1982**, *294*, 1317.
(44) Guiselin, O. *Europhys. lett.* **1992**, *17*, 225–230.
(45) Senden, T. J. *Curr. Opin. Colloid Interface Sci.* **2001**, *6*, 95.
(46) Lindstrom, T.; Wagberg, L.; Larsson, T. *Transactions of the 13th Fundamental Research Symposium of the Pulp and Paper Fundamental Research Society, Cambridge, U.K., 2005*; Pulp and Paper Fundamental Research Society: Cambridge, U.K., 2005; pp 457−562.

AM900096C